Arch. Metall. Mater. **71** (2026), 2, 459-464

DOI: https://doi.org/10.24425/amm.2026.158824

H.I. MAZLAN[1], N.H. OSMAN[1,2*], M.M. RAMLI[3], J.Y.C. LIEW[1,2], N.N. MAZU[1], M.A.H.M.A. MAJID[1,2], ALI H. RESHAK[4,5], B. JEŻ[6]

IMPACT ON LOW CONCENTRATION OF f-MWCNTs/Fe_3O_4 HYBRID FILLER ON ELECTROMAGNETIC INTERFERENCE (EMI) SHIELDING POLYMER AT X-BAND

Preventing electromagnetic interference (EMI) signals from interfering with sensitive electronic devices can help protect it from damage. A lightweight, flexible, and thin EMI shielding polymer provides an alternative to the conventional rigid and heavy metal gasket. In this work, the f-MWCNTs/Fe_3O_4 hybrid filler was synthesised using the co-precipitation method and used as filler for the EMI shielding polymer. Low-concentration filler of less than 1% was seen as the solution to reduce production costs. Thus, this work used only 0.1 w/v% and 0.5 w/v% of filler concentration of the f-MWCNTs/Fe_3O_4 hybrid filler. Raman's spectroscopy study confirmed the presence of carbon and Fe_3O_4 at 1200 to 1600 cm^{-1} and 686 cm^{-1} in the fillers, respectively. Examining the sample's morphology indicates the filler's length, diameter, and dispersion throughout the polymer. Electrical properties were studied using impedance spectroscopy, and EMI shielding effectiveness was measured using two-port methods. Results show that shielding polymer with 0.5 w/v% of f-MWCNTs/Fe_3O_4 hybrid filler results in 3.81×10^{-5} Scm^{-1} of electrical conductivity and 5.02 dB total shielding efficiency equivalent to 68.5% EM energy reduction. The total shielding efficiency increased to 8.32 dB (85.34% EM power shield) when the polymer thickness increased to 0.442 mm.

Keywords: Hybrid material; EMI shielding effectiveness; impedance spectroscopy

1. Introduction

Electromagnetic interference (EMI) is an unwanted electromagnetic signal that can interfere with other electronic devices. Protection against the EMI was important for sensitive electronic devices such as biomedical equipment, communication systems, computers, and radar systems [1-4]. The risk of EMI can be reduced by using shielding material with good electrical and magnetic properties. Conventionally, metals are used as EMI shielding due to their excellent electrical conductivity. Although metal has suitable EMI shielding properties, it has several limitations, such as high mass density, rigidity, and being prone to corrosion [5,6]. Polymer that offers good EMI shielding is an alternative due to its lightweight, thin, and flexible characteristics. Most polymers are electrical insulators in their natural state [7], but enhancing polymers with selected fillers may improve their electrical conductivity and magnetic properties. Polymer thickness also affects the shielding ability. The greater the thickness of the polymer, the more effective it is at shielding EMI. However, making it thicker reduced its flexibility. As a result, the thin layer of polymer with a high EMI shielding effectiveness was preferred.

Magnetite and carbon-based have been studied for various EMI shielding applications. Fe_3O_4 is known for its good magnetic properties, which make it an excellent potential filler to enhance the polymer's shielding efficiency. Carbon nanotubes (CNT) have excellent tensile strength and electrical and thermal properties [8-10]. An increase of up to 50% in EMI shielding efficiency with the addition of Fe_3O_4 and MWCNTs has also been reported [11].

This work is based on previous studies on magnetite and carbon-based materials for EMI shielding applications. This

[1] UNIVERSITI PUTRA MALAYSIA (UPM), DEPARTMENT OF PHYSICS, FACULTY OF SCIENCE, APPLIED ELECTROMAGNETIC LABORATORY 1, SERDANG 43400, SELANGOR, MALAYSIA
[2] UNIVERSITI PUTRA MALAYSIA (UPM), INSTITUTE OF NANOSCIENCE AND NANOTECHNOLOGY, NANOMATERIALS SYNTHESIS AND CHARACTERIZATION LABORATORY, SERDANG 43400, SELANGOR, MALAYSIA
[3] UNIVERSITI MALAYSIA PERLIS, INSITUTE OF NANO ELECTRONIC ENGINEERING (INEE), 01000 KANGAR, PERLIS
[4] UNIVERSITY OF BASRAH, PHYSICS DEPARTMENT, COLLEGE OF SCIENCE, BASRAH POST CODE 61004, IRAQ
[5] CZECH TECHNICAL UNIVERSITY IN PRAGUE, FACULTY OF MECHANICAL ENGINEERING, DEPARTMENT OF INSTRUMENTATION AND CONTROL ENGINEERING, TECHNICKA 4, PRAGUE 6 166 07, CZECH REPUBLIC
[6] CZESTOCHOWA UNIVERSITY OF TECHNOLOGY, FACULTY OF MECHANICAL ENGINEERING AND COMPUTER SCIENCE, DEPARTMENT OF TECHNOLOGY AND AUTOMATION, 19C. ARMII KRAJOWEJ AV., 42-200 CZESTOCHOWA, POLAND

* Corresponding author: nurulhuda@upm.edu.my

includes synthesising and characterising a free-standing EMI shielding polymer with a low f-MWCNTs/Fe_3O_4 hybrid filler concentration. The structural characterisation of the polymer composites was studied through Raman Spectroscopy and Scanning Electron Microscopy (SEM), along with their electrical properties and shielding abilities. The results showed that the polymer composite with only 0.5 w/v% of f-MWCNTs/Fe_3O_4 hybrid filler produced a high shielding efficiency of 5.02 dB and can be further increased to 8.32 dB by increasing the polymer thickness. This corresponds to an increment from 68.74% to 85.34% of the EM energy shield.

2. Experimental details

Ammonia solution was purchased from HmbG Chemicals. $FeCl_2.4H_2O$, $FeCl_3.6H_2O$, chitosan powder (medium molecular weight, 75-85% deacetylation), and acetic acid (99% purity) were all bought from Sigma Aldrich. MWCNTs were obtained from Tsinghua-Nafine Nano-Powder Commercialization Eng. Centre, China. As in previous work, the MWCNTs were functionalised by the acid functionalisation process [12].

Co-precipitation was used for the f-MWCNTs/Fe_3O_4 hybrid filler preparation [13]. The f-MWCNTs (200 mg), $FeCl_3 \cdot 6H_2O$ (176 mg), and $FeCl_2 \cdot 4H_2O$ (130 mg) were mixed in deionised water (250 ml) and were stirred for 10 minutes at 200 rpm at room temperature. The pH level of the mixture was increased to pH 11 by drop-wise addition of ammonia solution, causing Fe_3O_4 to precipitate. The mixture was stirred for 2 hours before being centrifuged to separate the water and solids. The mixture was dried to obtain f-MWCNTs/Fe_3O_4 hybrid filler with a ratio of 1:1. The same procedure was followed to synthesise pure Fe_3O_4 powder with f-MWCNTs excluded from the synthesis process.

The procedure continues with the preparation of the polymer solution using the solvent casting method [14]. Chitosan powder (1g) was diluted in acetic acid solution (2v/v%) before the addition of glycerol (2 v/v%). Glycerol acts as a plasticiser agent, improving the chitosan polymer's mechanical properties [15,16]. The f-MWCNTs/Fe_3O_4 (0.1 w/v% and 0.5 w/v%) were dispersed in deionised water before being added to the chitosan solution and stirred for 24 hours. The ready mixture was dried in the oven at 60°C for 24 hours. For comparison, chitosan polymers with only Fe_3O_4 (0.05 w/v% and 0.25 w/v%) were also produced, along with a control sample of pure chitosan polymer.

The electrical impedance of the polymer composite was measured using the programmable LCR Bridge (Rohde & Schwarz Hames, HM8118). Based on the bulk resistance (R_B) obtained from the Nyquist plot, conductivity (σ) was calculated using Eq. (1), where t is the polymer thickness, and A is the area of the electrode plate.

$$\sigma = \frac{t}{R_B A} \tag{1}$$

Real (ε') and imaginary (ε'') parts of permittivity can also be calculated from the impedance data using Eq. (2) and Eq. (3). Z' and Z'' are the real and imaginary parts of the impedance, ω is the angular frequency, and C_o is the capacitance of the free electrode. The ε' refers to the material's ability to store electrical energy, while ε'' is the dissipation of electrical energy from the material.

$$\varepsilon' = \frac{Z''}{\omega C_o \left(Z'^2 + Z''^2 \right)} \tag{2}$$

$$\varepsilon'' = \frac{Z'}{\omega C_o \left(Z'^2 + Z''^2 \right)} \tag{3}$$

The sample electromagnetic interference (EMI) shielding effectiveness was evaluated by placing the material between two waveguide ports connected to a Vector Network Analyser (Agilent 8720B) operating within the 8 to 12 GHz frequency range. The complex scattering parameters (or S-parameters) were obtained from this measurement and can be conveniently related to reflectance (R), transmittance (T) and absorbance (A) as shown in Eqs. (4) to (6).

$$T = |S_{12}|^2 = |S_{21}|^2 \tag{4}$$

$$R = |S_{11}|^2 = |S_{22}|^2 \tag{5}$$

$$A = 1 - R - T \tag{6}$$

The shielding effectiveness can be represented as shielding effectiveness due to reflectance (SE_R), absorbance (SE_A), and total shielding effectiveness (SE_T). Eqs. (7) and (8) show ways to determine the value of SE_R and SE_A. The total value of EMI shielding effectiveness was obtained by adding SE_R and SE_A as in Eq. (9).

$$SE_R = 10 \log_{10} \frac{1}{1-R} \tag{7}$$

$$SE_A = 10 \log_{10} \frac{1-R}{T} \tag{8}$$

$$SE_T = SE_R + SE_A \tag{9}$$

Furthermore, the conductivity and permeability influence the SE_R and SE_A as shown in Eqs. (10) and (11) [14].

$$SE_R = -10 \log_{10} \frac{\sigma}{16 \omega \mu \varepsilon_0} \tag{10}$$

$$SE_A = -8.86t \frac{\sqrt{f \mu \sigma}}{2} \tag{11}$$

3. Results and discussion

3.1. Raman Spectroscopy

Material identification was conducted using a Raman Microscope (XploRA Plus, Horiba). Fig. 1 shows three high-

intensity bands at approximately 1325 cm^{-1}, 1570 cm^{-1}, and 2650 cm^{-1}, known as D, G, and 2D bands. The D band indicates the disordered graphite structure, which refers to sp^3 used, such as the number of defects, while the G band indicates the good organisation of carbon material, which relates to sp^2 [17]. The intensity ratio of the bands (I_D/I_G) was used to calculate the amount of defective carbon material. Due to their high graphitic content, carbon-based materials such as f-MWCNTs always display a high-intensity G band. I_D/I_G ratio value of the f-MWCNTs/Fe_3O_4 hybrid was found to be 0.92, compared to f-MWCNTs measured at 1.841 [12]. Thus, more defects are present than in the filler, although it has a high graphitic level. Furthermore, the 2D band represents the multi-layered structure of f-MWCNTs and may suggest some broken structure of MWCNTs after undergoing the functionalisation process during synthesis. Meanwhile, a low-intensity band seen at 686 cm^{-1} confirms the existence of Fe_3O_4 in the hybrid mixture [18].

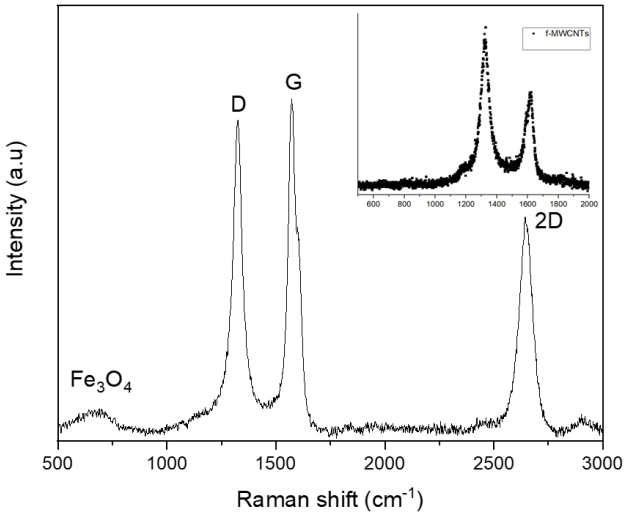

Fig. 1. Raman spectroscopy patterns of f-MWCNTs/Fe_3O_4 hybrid and f-MWCNTs (insert)

3.2. Scanning Electron Microscopy (SEM)

The surface morphology of the shielding polymer was studied using a Tabletop Surface Electron Microscope (HITACHI, TM4000Plus). Figs. 2(a) and 2(b) show the SEM images for f-MWCNTs/Fe_3O_4/Ch and Fe_3O_4/Ch polymer composite with uniform Fe3O4 and f-MWCNTs observed distribution. The average particle size analysis was determined using ImageJ software. From the analysis, the average Fe_3O_4 particle diameter in the Fe_3O_4/Ch polymer composite was approximately 5.45 µm, as shown in Fig. 2(a). The average f-MWCNTs particle length in f-MWCNTs/Fe_3O_4/Ch shielding polymer was approximately 1.83 µm, as shown in Fig. 2(b). The shorter length of f-MWCNTs can be attributed to the sonication process during the filler preparation, which would break the CNT [19]. This is in agreement with the Raman spectroscopy results, where the appearance of the 2D band suggested broken structures of the MWCNTs. The average Fe_3O_4 particle diameter in the f-MWCNTs/Fe_3O_4/Ch polymer was approximately the same as in the Fe_3O_4/Ch polymer. The well dispersed f-MWCNTs in the f-MWCNTs/Fe_3O_4/Ch polymer would lead to the formation of a conductive pathway that will contribute to higher conductivity in the samples.

3.3. Electrical Impedance Spectroscopy (EIS)

Fig. 3 shows the Nyquist plot for shielding polymers with different fillers and concentrations. All polymers show a similar trend with spikes and the onset of semicircles. The bulk resistance (R_B) of individual polymers, determined from the intersection of the semicircle and residual spike, was tabulated in TABLE 1. The Pure Ch has no conductive filler and produces the highest R_B value at 4.45 kΩ, resulting in the lowest conductivity of 4.45×10^{-6} Scm^{-1}. The addition of filler lowers the R_B and increases the conductivity. Adding Fe_3O_4 filler

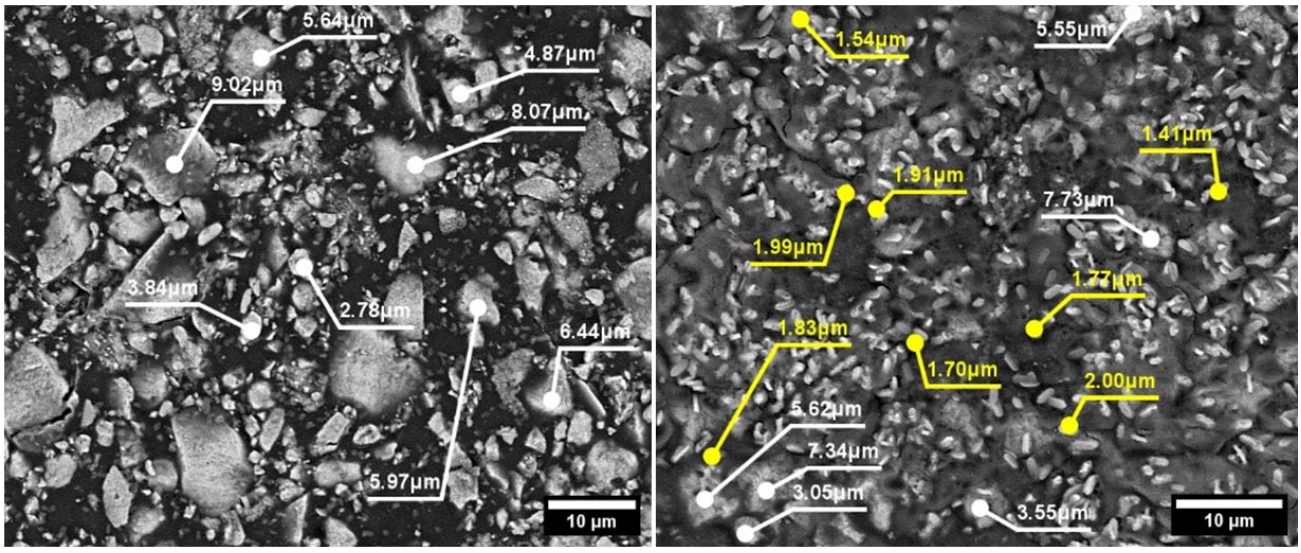

(a) (b)

Fig. 2. Morphology images for shielding polymer of (a) Fe_3O_4/Ch (0.25 w/v%) with 1000× magnification and (b) f-MWCNTs/Fe_3O_4/Ch (0.5 w/v%) with 1000×

at 0.25 w/v% increased the conductivity to 1.11×10^{-5} Scm^{-1}. The f-MWCNTs/Fe_3O_4 hybrid filler at 0.5 w/v% shows the highest conductivity of 3.81×10^{-5} Scm^{-1}. This is approximately triple the conductivity value compared to Fe_3O_4/Ch filler due to the excellent conductivity and distribution of f-MWCNTs as shown in Fig. 2(b).

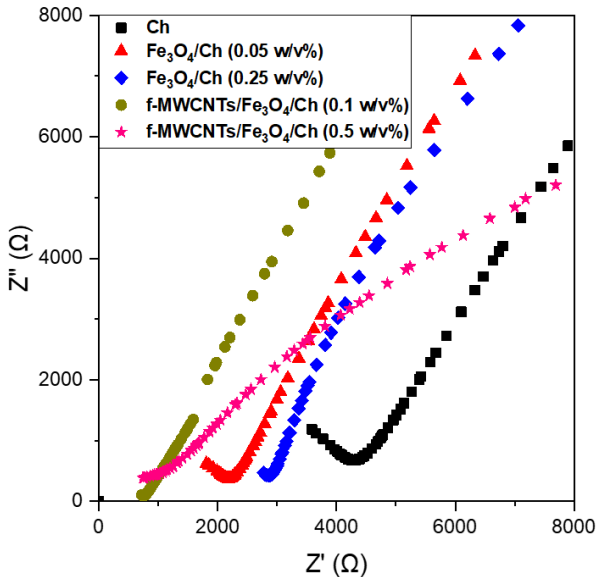

Fig. 3. Nyquist plot for Ch, Fe_3O_4/Ch and f-MWCNTs/Fe_3O_4/Ch shielding polymers

TABLE 1

Conductivity of Ch, Fe3O$_4$/Ch polymers, and f-MWCNTs/Fe_3O_4/Ch shielding polymers

Type of polymer	Filler concentration (w/v%)	Thickness (mm)	R_B (Ω)	Conductivity (Scm^{-1})
Ch	—	0.126	4450	4.45×10^{-6}
Fe_3O_4/Ch	0.05	0.153	2400	1.00×10^{-5}
Fe_3O_4/Ch	0.25	0.209	2950	1.11×10^{-5}
f-MWCNTs/Fe_3O_4/Ch	0.1	0.177	848	3.28×10^{-5}
f-MWCNTs/Fe_3O_4/Ch	0.5	0.221	912	3.81×10^{-5}

3.4. Dielectric permittivity

The real and imaginary parts of the complex permittivity, representing the dielectric constant (ε') and dielectric loss (ε''), respectively, are shown in Fig. 4. As observed in Figs. 4(a) and 4(b), both ε' and ε'' increase in the order of Ch < Fe_3O_4/Ch < f-MWCNTs/Fe_3O_4/Ch, reflecting the increased in the ability of the composites to store and dissipate electrical energy. This tendency corresponds to improved polarisation and conductive loss mechanisms introduced by incorporating magnetic and conductive fillers [20]. The observed increase in ε'' indicates higher energy dissipation through conduction losses due to the formation of effective charge transport pathways within the composite, which agrees with the increased electrical conductivity observed in the samples. Additionally, both ε' and ε'' exhibit higher values at lower frequencies and decline with increasing frequency, a typical behaviour of dielectric relaxation. This is attributed to more substantial polarisation effects and the accumulation of mobile ions at lower frequencies, contributing to interfacial polarisation and higher dielectric response. Dielectric losses are further associated with absorbing electrical energy used to rotate dipolar molecules within the polymer [21].

3.5. EMI shielding effectiveness

Figs. 5(a) to 5(c) shows the SE_R, SE_A, and the SE_T measured across the 8 to 12 GHz. The baseline chitosan polymer exhibits minimal SE_R and SE_A, as observed in Figs. 5(a) and 5(b). This is due to its intrinsically low electrical conductivity (σ) and magnetic permeability (μ), both critical parameters governing EMI shielding performance.

As described by Eqs. (10) and (11), SE_A is primarily influenced by dielectric and magnetic losses within the polymer composite, which are functions of both σ and μ. The SE_R, on the other hand, is predominantly dependent on the impedance mismatch between the polymer composite and the incident wave, which increases with higher electrical conductivity.

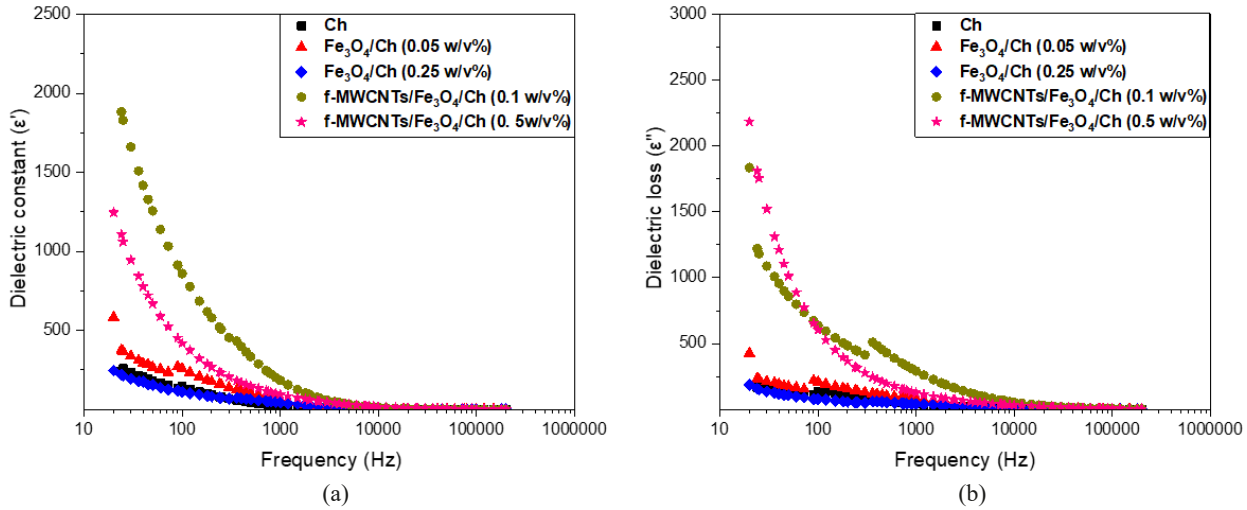

Fig. 4. (a) Dielectric constant and (b) dielectric loss for Ch, Fe_3O_4/Ch and f-MWCNTs/Fe_3O_4/Ch polymers

The incorporation of Fe_3O_4, confirmed via the Raman peak at 686 cm^{-1} as shown in Fig. 1, enhances the composite's permeability, thus facilitating magnetic loss and contributing to higher SE_A. The inclusion of the f-MWCNTs significantly increased the conductivity of the composite, as shown in TABLE 1, improving both SE_R through enhanced reflection and SE_A via increased dielectric loss. Furthermore, from the SEM image shown in Fig. 2(b), the f-MWCNTs were observed to be homogeneously dispersed on the surface of the chitosan composite, promoting the formation of a continuous conductive network. This uniform dispersion increases the impedance mismatch at the interface between the composite and the incident wave and contributes to higher shielding efficiency from higher reflection.

The overall effect of improved magnetic permeability and electrical conductivity is most evident in the f-MWCNTs/Fe_3O_4/Ch (0.5 w/v%) composite, which demonstrates superior shielding efficiency with SE_R of 1.81 dB, an average SE_A of 3.21 dB, and a resultant average SE_T of 5.02 dB. This confirms the critical role of both σ and μ in optimising EMI shielding efficiency in polymer composites.

While the filler loading was less than 1 w/v% and the composite thickness was below 0.5 mm, the resulting EMI shielding performance was notably high. The total shielding effectiveness can be further improved by increasing the filler concentration, enhancing the composite's electrical conductivity, magnetic permeability, and dielectric permittivity parameters. These parameters directly correlated with improved reflection and absorption mechanisms in EMI shielding materials.

TABLE 2

Average total shielding effectiveness (SET) with different filler concentrations and thicknesses

Type of polymer	Filler concentration (w/v%)	Thickness (mm)	Average SE_T (dB)
Fe_3O_4/Ch	0.05	0.153	1.05
Fe_3O_4/Ch	0.05	0.306	1.76
Fe_3O_4/Ch	0.25	0.209	1.61
Fe_3O_4/Ch	0.25	0.418	2.31
f-MWCNTs/Fe_3O_4/Ch	0.1	0.177	1.35
f-MWCNTs/Fe_3O_4/Ch	0.1	0.354	3.15
f-MWCNTs/Fe_3O_4//Ch	0.5	0.221	5.02
f-MWCNTs/Fe_3O_4/Ch	0.5	0.442	8.32

The shielding efficiency can be further increased by increasing the thickness of the shielding polymer. Comparisons of average SE_T with different thicknesses to study its relationship have also been made in this work. As shown in TABLE 2, the polymer's thickness contributes significantly to the SE_T values, where a thicker sample corresponds to higher EMI shielding effectiveness. This is because increased thickness extends the

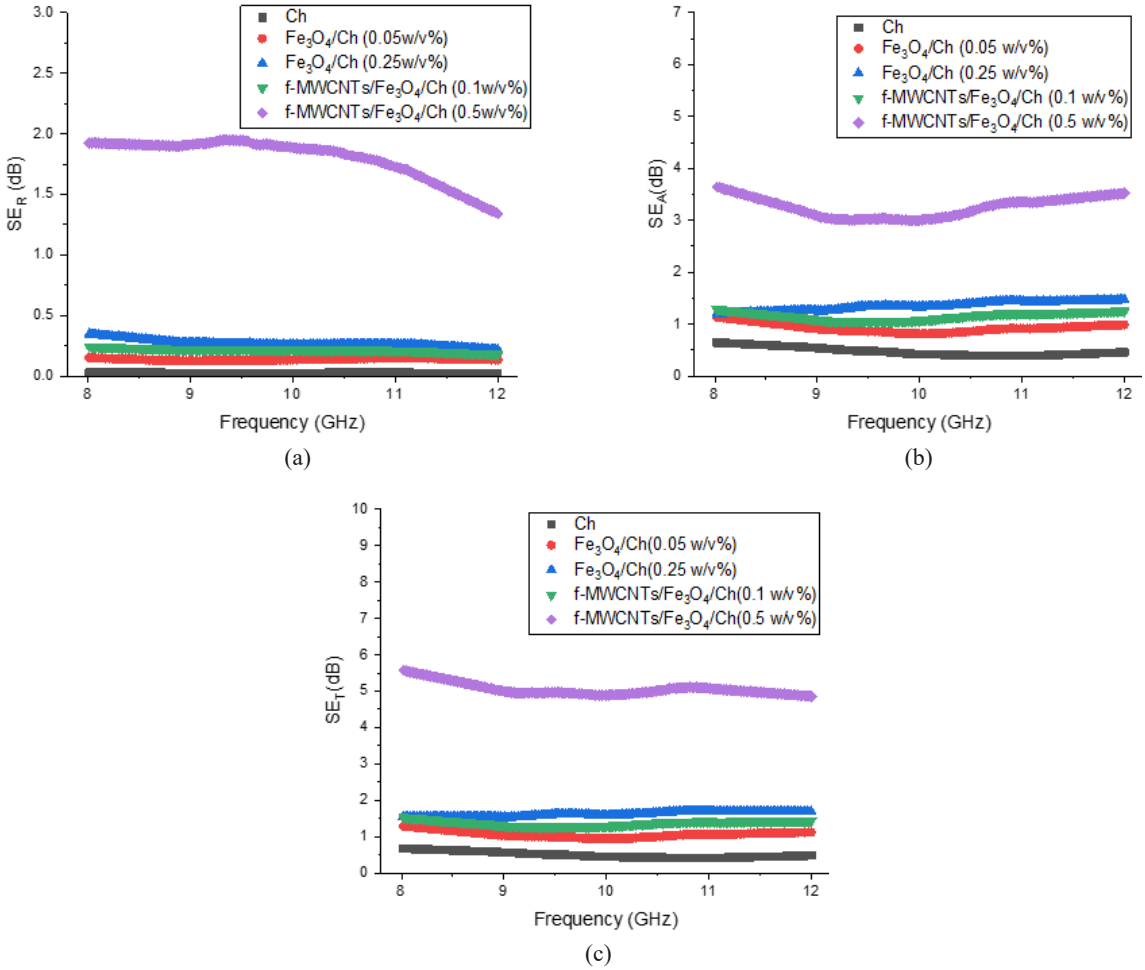

Fig. 5. SE_R (a), SE_A (b) and SE_T (c) for Ch, Fe_3O_4/Ch and f-MWCNTs/Fe_3O_4/Ch shielding polymer

propagation path of the electromagnetic waves within the polymer composite, thereby enhancing multiple internal reflections and increasing the probability of energy dissipation through absorption mechanisms. Doubling the thickness of f-MWCNTs/Fe_3O_4/Ch (0.5 w/v%) from 0.211 mm to 0.422 mm increased the SE_T from 5.02 dB to 8.32 dB on average, corresponding to 68.74% to 85.34% EM power shielded.

4. Conclusion

The EMI shielding polymer with low concentrations of f-MWCNTs/Fe_3O_4 using the casting method has been successfully prepared. The Raman spectroscopy results show high graphitic content with an ID/IG ratio value of 0.92 and represent the 2D band, suggesting a modification to the f-MWCNTs happened due to the hybridisation processes with Fe_3O_4. The SEM image shows good filler distribution in the film with an average size of f-MWCNTs of 1.83 μm. The electrical results show an increment in conductivity value in the f-MWCNTs/Fe_3O_4 film. This led to higher shielding recorded in the samples. The f-MWCNTs/Fe_3O_4 hybrid filler at 0.5 w/v% concentration in chitosan polymer produced 5.02dB total EMI shielding (68.74% EM power shield) at only 0.221 mm thickness. Moreover, the total shielding efficiency increased to 8.32 dB (85.34% EM power shield) when the thickness increased to 0.442 mm. It shows that even though a low filler is used, it can still produce high shielding efficiency.

Acknowledgements

This research was funded by the Ministry of Higher Education under the Fundamental Research Grant Scheme (FRGS/1/2023/STG05/UPM/02/10).

REFERENCES

[1] S.M. Zachariah, T. Antony, Y. Grohens, S. Thomas, From waste to wealth: A critical review on advanced materials for EMI shielding. Journal of Applied Polymer Science **139** (40), e52974 (2022).

[2] A. Kausar, et al., Nanocomposite foams of polyurethane with carbon nanoparticles – Design and competence towards shape memory, electromagnetic interference (EMI) shielding, and biomedical fields. Crystals **13** (8), 1189 (2023).

[3] L. Kong, et al., Recent progress in some composite materials and structures for specific electromagnetic applications. International Materials Reviews **58** (4), 203-259 (2013).

[4] Y. Chen, et al., Enhanced electromagnetic interference shielding efficiency of polystyrene/graphene composites with magnetic Fe3O4 nanoparticles. Carbon **82**, 67-76 (2015).

[5] H. Abbasi, M. Antunes, J.I. Velasco, Recent advances in carbon-based polymer nanocomposites for electromagnetic interference shielding. Progress in Materials Science **103**, 319-373 (2019).

[6] R.K. Bheema, K. Bhaskaran, A. Verma, M. Chavali, K.C. Etika, A Review on recent progress in polymer composites for effective electromagnetic interference shielding properties-Structures, Process, Sustainability approaches. Nanoscale Advances (2024).

[7] R. Rohini, S. Bose, Electromagnetic wave suppressors derived from crosslinked polymer composites containing functional particles: potential and key challenges. Nano-Structures& Nano-Objects **12**, 130-146 (2017).

[8] B. Peng, et al., Measurements of near-ultimate strength for multiwalled carbon nanotubes and irradiation-induced crosslinking improvements. Nature nanotechnology **3** (10), 626-631 (2008).

[9] B.Q. Wei, R. Vajtai, P.M. Ajayan, Reliability and current carrying capacity of carbon nanotubes. Applied Physics Letters **79** (8), 1172-1174 (2001).

[10] E. Pop, D. Mann, Q. Wang, K. Goodson, H. Dai, Thermal conductance of an individual single-wall carbon nanotube above room temperature. Nano Letters **6** (1), 96-100 (2006).

[11] A. Radoń, P. Włodarczyk, A. Drygała, D. Łukowiec, Electrical properties of epoxy nanocomposites containing Fe_3O_4 nanoparticles and Fe3O4 nanoparticles deposited on the surface of electrochemically exfoliated and oxidised graphite. Applied Surface Science **474**, 66-77 (2019).

[12] M.M. Ramli, S.S.M. Isa, S.J. Henley, Fabrication of multi-walled carbon nanotubes hydrogen sensor on plastic. In RSM 2013 IEEE Regional Symposium on Micro and Nanoelectronics (p. 316-319) (2013).

[13] K. Yu, et al., rGO/Fe_3O_4 hybrid induced ultra-efficient EMI shielding performance of phenolic-based carbon foam. RSC Advances **9** (36), 20643-20651 (2019).

[14] N.H. Osman, et al., Sodium-Based Chitosan Polymer Embedded with Copper Selenide (CuSe) Flexible Film for High Electromagnetic Interference (EMI) Shielding Efficiency. Magnetochemistry **7** (7), 102 (2021).

[15] P. Chen, F. Xie, F. Tang, T. McNally, Glycerol plasticisation of chitosan/carboxymethyl cellulose composites: Role of interactions in determining structure and properties. International Journal of Biological Macromolecules **163**, 683-693 (2020).

[16] S.Y. Park, K.S. Marsh, J.W. Rhim, Characteristics of different molecular weight chitosan films affected by the type of organic solvents. Journal of Food Science **67** (1), 194-197 (2002).

[17] . N. Coleman, U. Khan, W.J. Blau, Y.K. Gun'ko, Small but strong: a review of the mechanical properties of carbon nanotube–polymer composites. Carbon **44** (9), 1624-1652 (2006).

[18] P.C. Panta, C.P. Bergmann, Raman spectroscopy of iron oxide of nanoparticles (Fe_3O_4). J. Mater. Sci. Eng. **5** (217), 2169-0022 (2015).

[19] G.J. Price, M. Nawaz, T. Yasin, S. Bibi, Sonochemical modification of carbon nanotubes for enhanced nanocomposite performance. Ultrasonics Sonochemistry **40**, 123-130 (2018).

[20] C. Rayssi, S.E. Kossi, J. Dhahri, K. Khirouni, Frequency and temperature-dependence of dielectric permittivity and electric modulus studies of the solid solution $Ca_{0.85}Er_{0.1}$ $Ti_{1-x}Co_{4x/3}O_3$ ($0 \leq x \leq 0.1$). RSC Advances **8** (31), 17139-17150 (2018).

[21] D.M.D.M. Prabaharan, K. Sadaiyandi, M. Mahendran, S. Sagadevan, Structural, optical, morphological and dielectric properties of cerium oxide nanoparticles. Materials Research **19**, 478-482 (2016).